

EFFECT OF ALUMINA AND TITANIUM NITRIDES INCLUSIONS ON MECHANICAL PROPERTIES IN HIGH ALLOYED STEELS

J. LECOMTE-BECKERS¹, J. TCHOUFANG TCHUINDJANG¹, R. GFHIRI²,
P. BOERAEVE², L. DE COLNET³ AND E. PIRARD³

University of Liège, Belgium

¹*Metallurgy & Material Sc. - ²MSM - B52/3, Chemin des Chevreuils 1, 4000 Liège, Belgium*

³*MICA laboratory - D2, Avenue des Tilleuls 45, 4000 Liège, Belgium*

ABSTRACT

Regardless of the melting or the atmosphere during the melting, inclusions are present in every commercial steel product in varying amounts. Since inclusions significantly influence properties and behaviour of materials and at the same time give indications on the quality of the steel, it is quite interesting to precise their nature and their origin.

In this paper concerning a project involved in the COST 517 framework, studied alloys are high alloy steels. The raw materials were obtained from the conventionally electrical cast ingot and the Electro Slag Refining processes.

The purpose is to compare various inclusions produced by these different processes and their effect on the mechanical properties. The raw material because of the melting processes themselves, leads to a product with a good to a great cleanliness, and tiny inclusions, which are haphazardly distributed. The actual ASTM E45 chart seems to be inappropriate, as the inclusions founded are too small in size. Therefore, we manage to develop a specific procedure for the study of such inclusions. The different types of inclusions encountered are oxides, titanium nitrides, and manganese sulphides.

Studying the effect on mechanical properties, oxides often seem to initiate fatigue fracture.

KEYWORDS

High alloyed steel, inclusion, fracture (initiation, propagation).

INTRODUCTION

The inclusion content is known to have a significant influence on fatigue life in hardened steels [1]. As experiments results, it is well established that size of inclusions is a critical fatigue life parameter [2]. Fatigue is the progressive, localized, and permanent structural change that occurs in a material subjected to repeated or alternating stresses. The level of the fatigue strength used to be lower than the tensile strength of the material.

From a theoretic point of view several others parameters are also expected to affect fatigue performance [3]. As examples of such parameters, we talk about the occurrence of crack inside inclusion, interface between inclusion and lattice, modulus and even expansion properties of the inclusion itself.

MATERIAL AND EXPERIMENTAL METHODS

Raw material

Raw material used was elaborated in the industrial plant, according to common industrial practice. After appropriated heat treatments and subsequent machining (forging at 1150°C in a direction parallel to roll axis), industrial applications of raw material are cold rolling-mill rolls.

Two processes are used for the melting: the conventional melting in electrical furnace with vacuum degassing (EF), and Electro Slag Refining (ESR). ESR is assumed to lead to a cleaner metal devoid of impurities.

The raw material is a tool steel, and the average chemical composition of the different types of the studied material is given here below (See Table 1).

Table 1: Average composition of the different types of the studied material, depending on the melting process.

<i>Melting process</i>	<i>Alloyed elements (% of weight)</i>							
	<i>C</i>	<i>Mn</i>	<i>Si</i>	<i>Cr</i>	<i>Mo</i>	<i>Ni</i>	<i>V</i>	<i>Cu</i>
ESR (2 Slags)*	0.8/1.0	0.1/0.4	0.7/1.0	4.7/5.2	0.1/0.3	0.2/0.5	Slight traces	0.1/0.3
EF**	0.8 /1.0	01/0.4	0.6/0.9	4.6/5.1	0.1/0.3	0.1/0.4	Slight traces	0.1/0.2

* Two slags are used in ESR process; they differ from one to another in their composition.

** In EF process, the steam melting is used with or without the presence of an inert gas.

Heat treatments

A specific heat treatment has been performed to insure that the microstructure on the whole batch of specimens of the same origin is similar. First, a preliminary heat treatment consisting both in homogenising and normalising the microstructure was done. The raw material went through the heat-treatment process of austenitisation at 900°C for 6 h, with a cooling rate controlled (between 10 to 15°C/min, before Ar₃). This heat treatment was done on primary blocks (2 blocks taken from the shell of the roll) and led to a fully fine lamellae pearlitic microstructure of about 250HV. Then a subsequent hardening was done on rough shaped samples, cut in a direction parallel to spindle roll (Block 1) and in a direction perpendicular to roll axis (Block 2). The hardening involves austenitisation at 950°C for 20 min, oil quenching to room temperature, and a double tempering at 100°C for 4h. The hardening is supposed to yield on each sample actual mechanical properties similar to that of the application (Rolls). Hardening leads to a fully martensitic structure, with a hardness of about 830 HV.

Experimental method

We use an electromechanical fatigue device fitted out with a 100 KN load cell. All tests were carried out with a 100Hz frequency and each test was run until failure or 10⁷ cycles. 15 samples were cut out of preliminary blocks after normalizing and rough shaped. The hardening was carrying out on samples (bulked by 5), and fatigue tests performed on shaped samples, after final machining. Figure 1 gives sizes of the sample for fatigue test.

The fatigue-test consists of applying a repeated stress on the sample, with a non-zero value for the minimum of the strength (70 MPa). The maximum value is haphazardly chosen. For a given sample, the number of cycles before fracture occurs is recorded. If this number reaches 10⁷ cycles without failure, we assume the lifetime of the sample to be infinite.

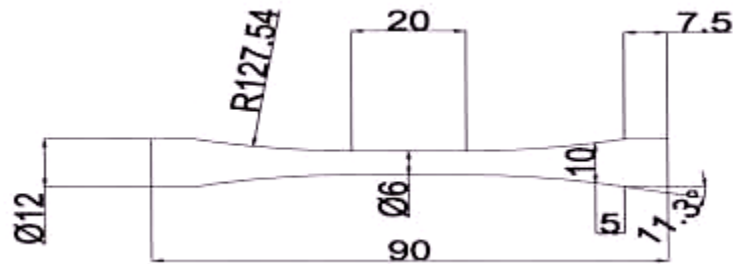


Figure 1: Dimensions of fatigue test specimen

RESULTS

Characterization of inclusions

All the samples have been analysed in the as-received conditions, for the characterization of inclusions. First we cut a 15 mm edge cube out of the raw material. Then the sample is encased in a hot polymeric resin, grinded and polished. Polished surface, which is to be studied, is then analysed without any etching, towards bright field optical microscopy.

Using a virtual framework, inclusions are marked out and classified into groups, according to appropriate parameters chosen for optical microscopy. Then we check the location of the leading inclusion of a group by the means of electron microscopy (SEM, EDX) to determine the nature of the inclusion. The networking is helpful for a rapid location of inclusions, which are to be analysed with SEM or EDX.

Table 2 here below gives a general idea of the different types of inclusions founded in the raw material, with distinctive features connected to the melting process itself. Some illustrations of inclusions, as they appear towards bright field optical microscopy, are given in figure 2 to figure 5.

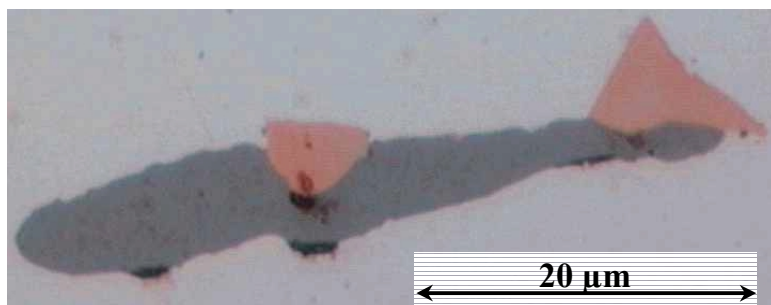


Figure 2: Mixed inclusion in EF-NOPRO
(TiN (Pink), MnS (Dove gray) and oxides (Dark))

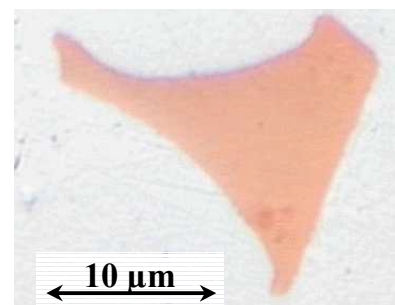


Figure 3: TiN in ESR-a

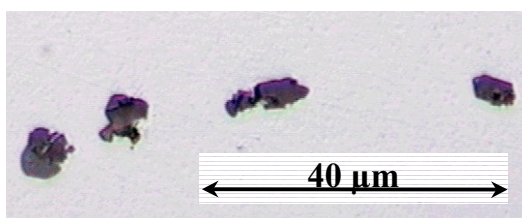


Figure 4: Stringer of oxides in ESR-a

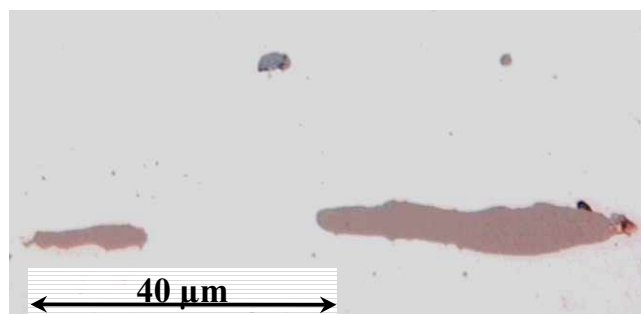


Figure 5: Sulfides stringer in EF-NOPRO

Table 2: Characterization of inclusions according to optical microscopy

<i>Feature</i>	<i>Titanium nitrides</i>	<i>Manganese sulphides</i>	<i>Oxides (Alumina, Aluminosilicates)</i>
Colour	Pink	Dove grey	Dark grey, Mauve or Dark
Shape	<ul style="list-style-type: none"> ◆ Angular (ESR) ◆ Angular and globular (EF) 	<ul style="list-style-type: none"> • Cigar shaped (ESR) • Globular, spheroid or elongated (EF) 	<ul style="list-style-type: none"> ♣ Angular (ESR) ♣ Angular and globular (EF)
Size	<ul style="list-style-type: none"> ◆ Up to 20 μ (ESR) (<i>< 10 μ, with ESR-b</i>) ◆ Up to 40 μ (EF) 	<ul style="list-style-type: none"> • Up to 40 μ (ESR) • Up to 100 μ (EF) 	<ul style="list-style-type: none"> ♣ Up to 5 μ (ESR) ♣ Up to 20 μ (EF) <i>(The larger ones are associated with sulphides)</i>
Quantity	<ul style="list-style-type: none"> ◆ High (ESR) ◆ High (EF) 	<ul style="list-style-type: none"> • Very low (ESR) (<i>The smaller average is obtained with ESR-b</i>) • Very important (EF) 	<ul style="list-style-type: none"> ♣ Low (ESR) ♣ High (EF)
Isolated	<ul style="list-style-type: none"> ◆ Often (ESR) ◆ Not usual (EF) 	<ul style="list-style-type: none"> • Often (ESR) • Not usual (EF) 	<ul style="list-style-type: none"> ♣ Rarely (ESR) (<i>Excepted for ESR-b</i>) ♣ Not usual (EF)
Association	<ul style="list-style-type: none"> ◆ Double with oxides (all), and triple (with both oxides and sulphides) (ESR) ◆ Double, especially with sulphides, or triple. <i>Triples are most commonly founded than double ones</i> (EF) 	<ul style="list-style-type: none"> • Double with oxides (ESR) • Doubles (with nitrides or oxides), and triples. <i>Triples are most commonly founded than double ones</i> (EF) 	<ul style="list-style-type: none"> ♣ With sulphides and nitrides (ESR) ♣ Doubles with sulphides, and triples. <i>Triples are most commonly founded than double ones</i> (EF)
Aggregates	<ul style="list-style-type: none"> ◆ More often in ESR-a than ESR-b ◆ Stringers and sometimes isolated (EF) 	<ul style="list-style-type: none"> • Larger in ESR-a than ESR-b. • Often bulk around a bigger inclusion. Stringers (EF) 	<ul style="list-style-type: none"> ♣ Alumina (ESR-b) and Aluminosilicates (bulky in ESR-a) ♣ Important (EF)

Inclusions as determined by SEM and EDX are of different types: titanium nitrides, manganese sulphides and complex oxides (alumina, aluminosilicates). Sometimes Ca appears to be associated to Mn in sulphides. Moreover Si is often associated to Al leading to complex oxides.

Inclusions can mainly be distinguished by optical microscopy throughout their colour: titanium nitrides are pink, manganese sulphides are grey to dove grey, and the oxides appear dark grey or mauve.

Despite their nature, inclusions appear two times smaller in size or even more, in samples elaborated by ESR process than they are in EF ones.

The most encountered aggregates are oxides, both in ESR and EF. Sulphides also form aggregates (ESR and EF), but aggregates of nitrides are encountered only in samples elaborated from EF process. Oxides aggregates appear as stringers of inclusions both in ESR and EF samples.

Results of fatigue tests

We assume the endurance limit to be the maximum level of the strength, which leads to achieve a number of cycles greater or equals to 10^7 cycles.

Results are presented on figure 7 here below. These results show a high dispersion in the fatigue behaviour, especially with samples of Block 2, where the direction of axis is perpendicular to the roll spindle.

There is a great difference in the endurance limit of samples depending on the direction of the sampling. In fact fatigue strength is greater when axis of samples is parallel to the forging direction (**900 MPa**) than the value obtained with samples cut out perpendicular to the spindle of the previous roll (**700 MPa**). There is a decrease of about 22% in the endurance limit when axis of samples is perpendicular to forging direction instead of being parallel to the same forging direction.

The studied material appears to be fragile. In fact we found cases where fracture occurs on several sections, leading to multiple sections on the sample (See fig. 6).



Figure 6: Multiple section fracture on a sample after fatigue test

General study of the fracture

In addition to the results of fatigue tests, we have analysed fracture surfaces in order to identify the origin of the failure. These examinations were done both with stereoscopic microscopy and scanning electron microscopy. In most of the cases, fracture seems to initiate near the surface of the sample, leading to a little circle relatively smooth around the origin: this is the so-called **initiation stage of the rupture**. And beyond this circular area, the appearance of the rupture changes with a set of concentric ridges converging at the fracture origin, which represents the **propagation stage of the rupture** (see figures 8 and 9). Figure 8 is obtained by the means of stereoscopic microscopy, while figures 9 and 10 come from SEM. Observation of fracture surface showed that in most of the cases fatigue fracture is initiated from a complex oxide and nitride inclusion.

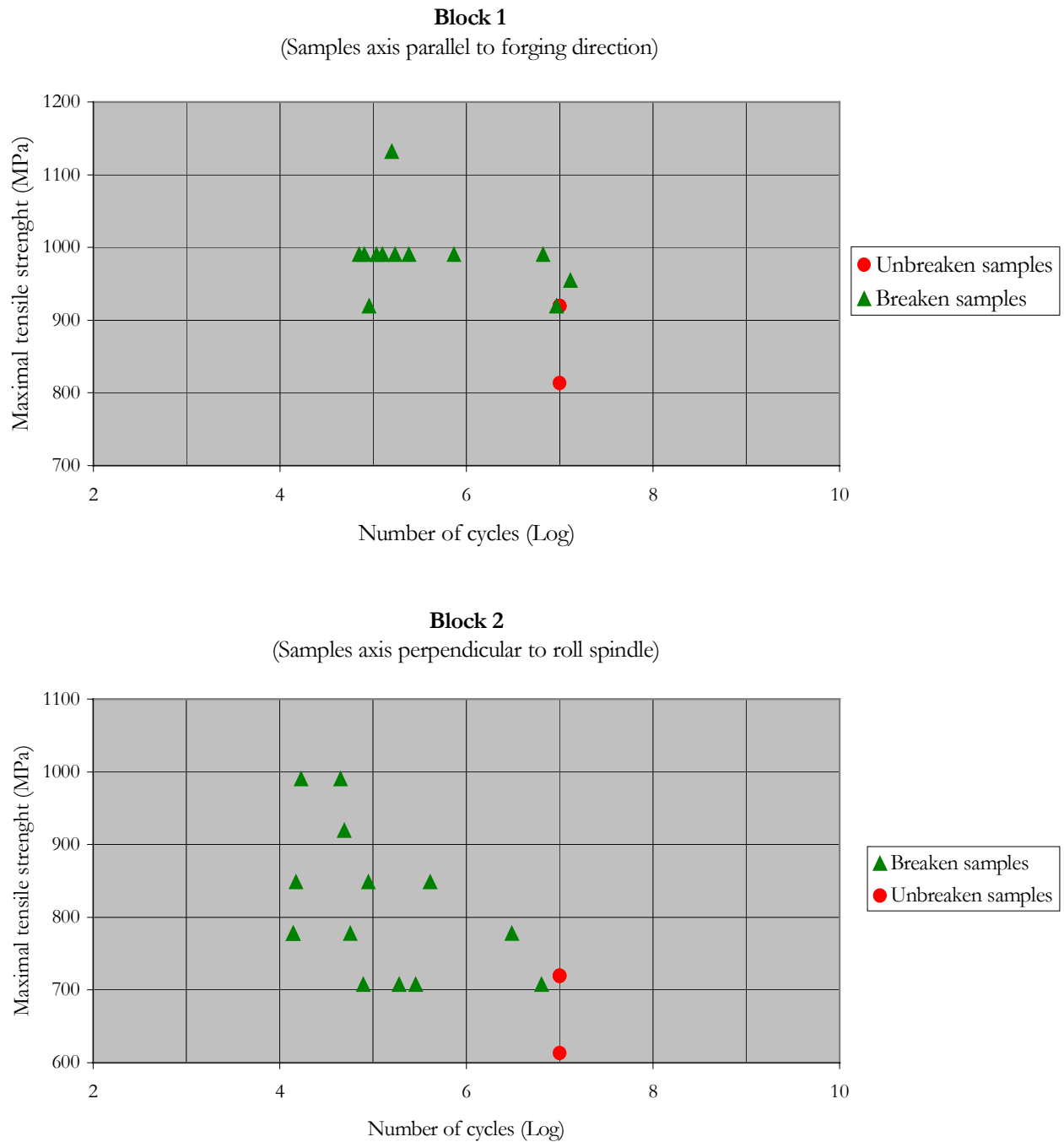


Figure 7: Results of the fatigue test
Samples with axis parallel to the roll spindle (above) and samples with axis
perpendicular to roll axis (below)

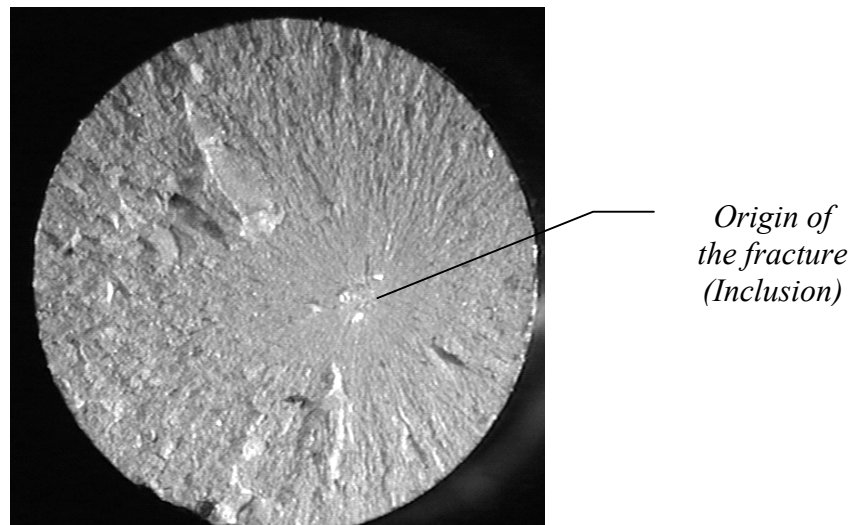


Figure 8: Broken section of a sample after fatigue test

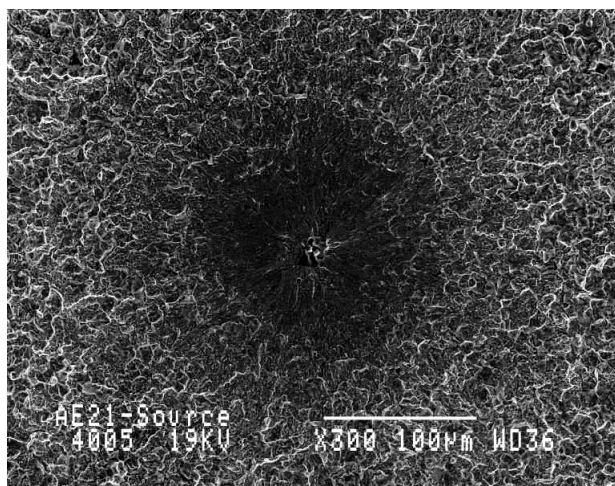


Figure 9: Broken section of a sample after fatigue test - Origin and initiation area of the fracture (Cylindrical dark area)

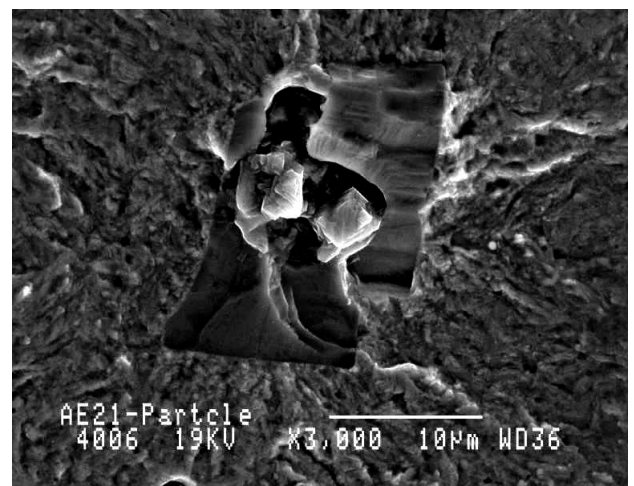


Figure 10: Inclusion as origin of the fracture (Mixed particle with Al, Si and Ti)

DISCUSSION AND CONCLUSION

We manage to develop a specific procedure for the study of inclusions encountered, as the actual ASTM E45 chart seems to be inappropriate. In fact, inclusions founded are too small in size. As a result, it seems obvious that the raw material, because of the melting processes themselves, leads to a product with a good to a great cleanliness, with tiny inclusions, which are haphazardly distributed.

Although Ti is not known as an alloyed element in the raw material itself, we found that there were a great amount of nitrides either in ESR or EF samples. We assume that the Ti, which fixes nitrogen to form nitrides, is already present in the melting environment before the process goes on.

However, TiN seems to be smaller in size in ESR than they are in EF. We infer that the refining of an electrical ingot by ESR process breaks large particles of TiN, which are redistributed in smaller particles.

In the case of a mixed inclusion, it is quite possible to infer the sequence of appearance of one type of inclusion in comparison with another one. In fact, the particle that appears firstly in a mixed inclusion is located in the core of the other one. It is the case with oxide, which can be located in the core of a titanium nitride.

When the origin of the failure in fatigue test is clearly defined somewhere on the section of the sample, the fracture is originated from an inclusion, and the region where the fracture initiates appears as circular area. The inclusion located at the origin of the rupture is often an oxide (alumina or aluminosilicate), or a mixed particle of oxide and nitride.

We found some cases where no origin was visible, the origin of the fracture being located at the surface of the sample. In the present circumstances, we cannot specify whether the fracture initiates on an inclusion located at the surface, or if the rupture appears as the result of a surface defect due to the previous machining.

In our case, there are several stages in the machining of the samples used (milling, turning and rectification). Actually, the way machining process is run could have a great effect on fatigue behaviour.

There is a great difference in the endurance limit depending on the direction of the forging. In fact fatigue strength is greater in a direction parallel to the forging axis than the value obtained in a direction perpendicular to the latter.

In order to establish the correlation between inclusions pattern and the behaviour of samples during fatigue test, we think that the assessment of all the inclusions founded on a polished area representing a sample diameter could be of great interest. In fact, the ratio of oxides founded on such a section could give the probability that the fracture occurs, and even the level of the endurance of the piece in use against repeated stresses. The work will be purchased in this way.

ACKNOWLEDGEMENTS

The authors thank the Society FORCAST (AKERS group) for the supplying of raw material and for useful discussions.

REFERENCES

- [1] J. MONNOT, B. HERITIER, and J. Y. COGNE - Relationship of melting practice, inclusion type and size with fatigue resistance of bearing steels: Effect of steel manufacturing processes on the quality of bearing steels - STP 987, 149-165, 1988 Philadelphia, PA, ASTM.
- [2] Y. MURAKAMI, S. KODAMA, and S. KONUMA - Int. J. Fatigue, 1989, 11, 291-307
- [3] A. MELANDER and A. GUSTAVSSON - Int. J. Fatigue, 1996, 18, 389-399